Mutual Coupling Reduction with a Novel Fractal Electromagnetic Band Gap Structure

Alaa H. Radhi[1], R. Nilavalan[1], Yi Wang[2], H. S. Al-Raweshidy[1], Amira A. Eltokhy[2], Nur Ab Aziz[1]

[1]College of Engineering, Design & Physical Science, Brunel University, London, UK.
[2]Department of Engineering Science, University of Greenwich, Chatham Maritime, Kent, UK.
Email: Alaa.Radhi@brunel.ac.uk

Abstract: This work shows the effect of a novel Fractal based Electromagnetic Band Gap (FEBG) structure between dual PIFAs antenna elements. The FEBG structure without any shorting pins builds on a well-known fractal structure called Sierpinski carpet, where two iterations have been applied as a uniplanar EBG between dual PIFAs elements to increase the isolation. The proposed antenna can operate at approximately 2.65 GHz for wireless Long Term Evolution (LTE) application with compact design dimensions. The simulations are carried out with Ansoft HFSS ver 17.0. The second iterative order FEBG band-gap characteristic is verified using more computationally efficient analysis. An investigation on coupling reduction showed more than 27 dB, and 40 dB in E-plane and H-plane; respectively between the dual antenna elements is achieved for an antenna spacing less than half wavelength. The proposed antennas with and without second iterative order FEBG are fabricated and measured. The measurement results are in good agreement with the simulated results. Moreover, the envelope correlation of antenna elements with the proposed FEBG is quite smaller than that of antenna elements without FEBG, which gives the proposed system an excellent diverse performance and suitable for the use in low-frequency narrow-band MIMO applications.

1. Introduction

Multiple-input, multiple-output (MIMO) systems can provide a significant increase in wireless channel capacity without the need for an additional spectrum or transmit power [1]. With the rapid expansion of wireless MIMO communication systems, the demand for low profile, wide bandwidth, and high isolation between antenna arrays has increased to maintain good diversity performance. Low mutual coupling (high isolation) between adjacent antenna elements is one of the essential requirements for any MIMO/diversity antenna implementation [2, 3]. Mutual coupling between closely spaced antennas is caused by radiation emission through electromagnetic coupling and conduction emission through a common conductor, such as the ground plane [1]. Efforts have been exerted to eliminate or decrease the effects of the mutual coupling between different microstrip antenna elements used in MIMO applications. In recent years, several techniques have been employed to achieve these objectives [4].

The main techniques that have been extensively studied and discussed in the literature for mutual coupling reduction are as follows: electromagnetic band gap (EBG) structures [2–7], defected ground plane structures [8–10], neutralization technique [11–13], slots and slits on the ground plane [14-16], insertion of a small ground plane between PIFA and PCB [17], T-shaped decoupling slots [18], spatial and angular variation techniques[19-22], addition of resonant slots [23], and planar soft surfaces [24]

EBG structures have been widely studied. These structures are considered efficient in reducing the mutual coupling between antennas due to their excellent filtering characteristics. Periodic structures, such as a Fractal-based EBG (FEBG), can suppress surface wave propagation in a particular frequency range. Currently, researchers worldwide have been combining fractal geometry with electromagnetic theory, which have resulted in a vast amount of new and innovative designs for mutual coupling reduction between different microstrip antenna elements working in MIMO applications [1]. In the literature, extensive research has been conducted using FEBG for mutual coupling reduction between various microstrip antennas [25-28]. Recently, fractals have been employed to numerous applications of modern MIMO antenna designs, such as compact antennas, mutual coupling reduction, filter applications, leakage suppression, and harmonic tuning for power amplifiers [26].

However, in the present work; fractal structures were utilised for mutual coupling reduction between microstrip antennas operating in a MIMO environment. FEBG structures have a unique property of compactness with long current paths where they can work efficiently in low-frequency range due to space-filling features. In addition, these fractal structures can provide a band-stop effect because of their self-similarity features for a particular frequency band; these filtering effects are due to the combination of inductance and capacitance [25]. Fractal geometry is mainly considered an appropriate technique in designing multiband and low-profile antennas. These fractal structures can also be utilised for mutual coupling reduction between different microstrip antennas operating in a MIMO environment. A new arrangement of FEBG structure is proposed to work with a stop band centred approximately at 2.6 GHz to reduce mutual coupling between dual PIFA antenna elements. With the aim of a small mobile handset application, the primary radiating patch of the antenna was designed to resonate at LTE radio frequency (f_r = 2.65 GHz) running in MIMO environment. The proposed antenna was fabricated, and practical measurements were conducted. The results of the simulations and measurements were in good agreement. The rest of this paper is organised as follows. Section 2 presents and analyses the geometry of antennas, configuration of the proposed FEBG structure, and band gap characteristics. Section 3 discusses the mutual coupling

reduction performance using the proposed FEBG. Other performance studies, such as simulated radiation patterns, are performed in this section. Section 4 explains the fabrication and measurements for the proposed antenna. A comparison between the simulated and measured results is also indicated in this section. Section 5 compares the proposed FEBG structure with other approaches and other recent studies. Finally, Section 6 provides the conclusions.

2. FEBG structure for coupling reduction

2.1. Fractal electromagnetic bandgap structure

Fractal structures comprise multiple small elements patterned after a self-similar object (with scaled-down designs) to maximize the physical length of current paths or redistribute the surface current density. These properties make these structures applicable at low-frequency ranges in wireless applications. Fractal structures have been widely studied in the literature. They provide multi-band operation, performance enhancement, and meets the miniaturisation requirements of mobile equipment [25, 29]. Meanwhile, the present study focuses on mutual coupling reduction using these compact fractal structures.

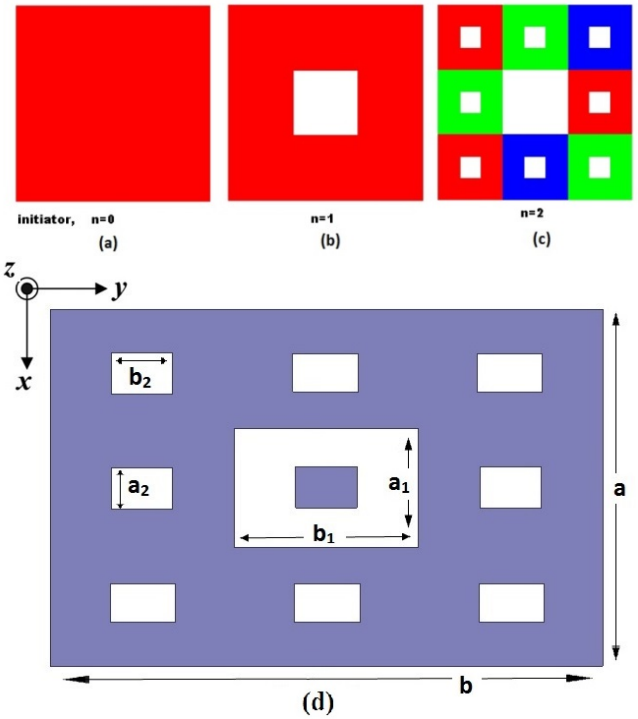

Fig. 1 *Illustration of the fractal geometry.* ***(a)*** *Zero-iteration order,* ***(b)*** *First-iteration order,* ***(c)*** *Second-iteration order,* ***(d)*** *Layout of the proposed second iterative order FEBG unit cell.*

The designed fractal geometries are zero, first, and second-order iterative structures based on a well-known fractal structure called Sierpinski carpet (as shown in Figs. 1(*a*)–1(c)). The zero-order iterative fractal structure is a single metallic (copper) square, as shown in Fig. 1(*a*). The first-order iterative fractal structure is divided into nine small congruent squares, where the open central square is dropped (n = 1), as shown in Fig. 1(*b*). The second-order iterative fractal structure evolves from first-order iterative fractal structure, as shown in Fig. 1(*c*). The remaining squares are divided into nine small congruent squares, in which each central square is dropped (n = 2). In this study, a well-known fractal type, Sierpinski carpet, is applied as a planar EBG structure between dual antenna (PIFA) elements to obtain a high isolation. In comparison with other structures (e.g., mushroom-like EBG) that occupy a large space between elements, FEBG structures have a more compact size and less complicated configuration (applicable without the use of Vias and does not require any shorting pins or other types of vertical connection) [30, 31].

Meanwhile, these properties are integrated easily with other radio frequency and microwave components, and relatively, they have a broader stopband bandwidth that provides an adequate surface wave suppression effect. Fig. 1(*d*) illustrates the proposed design of the second iterative order FEBG unit cell. The parameters optimisation based on scaling down with number of iterations by a particular factor (1/3) and the optimised parameters of the proposed second iterative order FEBG used in this work are:

$$a = 9\ mm, b = 13\ mm, a_1 = \frac{1}{3} \times a, b_1 = \frac{1}{3} \times b,$$

$$a_2 = \frac{1}{3} \times a_1\ ,\ b_2 = \frac{1}{3} \times b_1$$

The unit cells are etched on an FR_4 dielectric substrate with ε_r = 4.4 and thickness h =1.6 mm.

2.2. FEBG bandgap characteristics

The EBG with a periodic shape provides a rejection band in some frequency ranges. This bandgap filtering characteristic of EBG enables the mutual coupling reduction between antenna array elements. In the present work, the eigen mode analysis is performed using a full-wave simulation tool (HFSS software ver. 17.0) to demonstrate the filtering characteristics of the proposed second-order iterative FEBG structure. Different from transmission line method or reflection phase diagram, which responds to a normal wave incidence case, the dispersion diagram includes an EBG response for every possible incidence angle, thereby providing a complete picture of EBG frequency bandgaps [32, 33] considering that surface waves are mainly concentrated in the substrate and at the substrate/air interface [34]. However, the FEBG structure prevents surface wave propagation in a specific frequency band of interest for all incident wave angles and polarisation states.

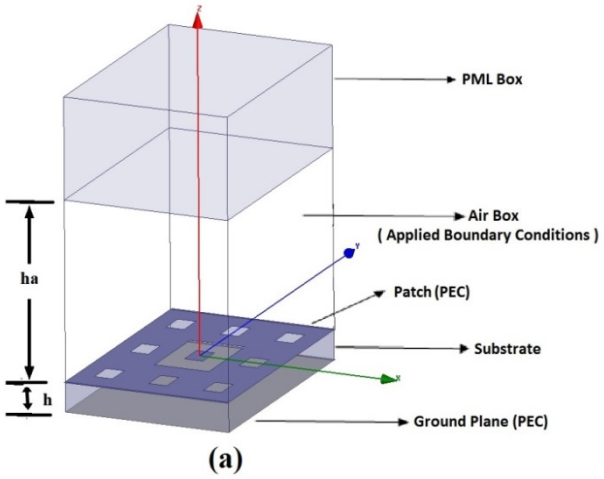

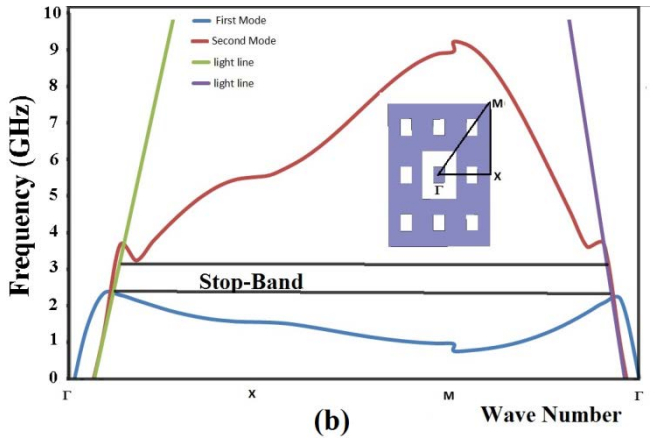

Fig. 2 (a) *FEBG unit cell with Perfect Matched Layer (PML) & Periodic Boundary Conditions (PBC) and* ***(b)*** *Dispersion diagram.*

In this work, an air column (*ha*) was placed above the dielectric substrate, and it was established at ten times the substrate height ($ha \simeq 10 \times h$) to emulate the free space over the structure as illustrates in Fig. 2(a). The dimensions of the FEBG unit cell are optimised to obtain rejection band between 2.5 GHz and 2.9 GHz. Fig. 2(*b*) illustrates the simulated dispersion diagram with a band gap between the first and second modes. The centre bandgap frequency of the proposed FEBG is f_c = 2.65 GHz approximately.

2.3. *Multiple antennas and FEBG structure*

The designed and fabricated antennas are shown in Fig. 3(*a*) and Fig. 3(*b-c*), respectively; without and with the proposed second iterative order FEBG structure.
The PIFA antenna elements working at f_c = 2.65 GHz are placed collinearly along the y-axis, and the space distance of these antennas is 40 mm from element centre to centre (corresponds $0.35\lambda_0$ at 2.65 GHz). The substrate of the proposed antenna is FR_4 with loss tangent (tan δ) = 0.02 and dielectric constant ε_r = 4.4 with appropriate 50 Ω coaxial connectors are used as the feed ports of the proposed PIFAs. Each PIFA element has a rectangular outline with a width *W* = 19 mm and patch length *L*=30 mm. The dimensions of the ground plane are 68 × 40 mm^2 (corresponds $0.6\ \lambda_0 \times 0.35\ \lambda_0$); other detailed dimensions are presented in Table 1.

Table 1 Detailed dimensions of the proposed antenna

Parameters	Values
Frequency (f_c)	2.65 GHz
Height of substrate (*h*)	1.6 mm
Ground length (*Lg*)	68 mm
Ground width (*Wg*)	40 mm
Patch length (*L*)	30 mm
Patch length (*W*)	19 mm
FEBG structure length (*Ls*)	39 mm
FEBG structure length (*Ws*)	18 mm
Distance (*D*)	5 mm
Space (*S*)	40 mm ($0.35\lambda_0$)
Shorting pin radius	0.3mm
Coaxial pin radius (Outer)	1.6 mm
Coaxial pin radius (Inner)	0.7 mm

The designed PIFA antenna is working in the higher-order mode. Optimisation was performed for the proposed diversity antennas to operate at a higher order mode to cover 2640–2680 MHz LTE band with best return loss characteristics as possible and at the same time have an appropriate load impedance matching without using an additional circuit of the proposed antennas.
The dimensions of the PIFAs, as well as other parameters such as feeding and shorting pins positions, were carefully fine-tuned with the help of the HFSS ver 17.0 electromagnetic software to obtain a required operational mode (higher-order mode) working at the frequency of interest. Through parameters sweep and optimisation, best antenna parameters have been achieved for maximising the isolation values.

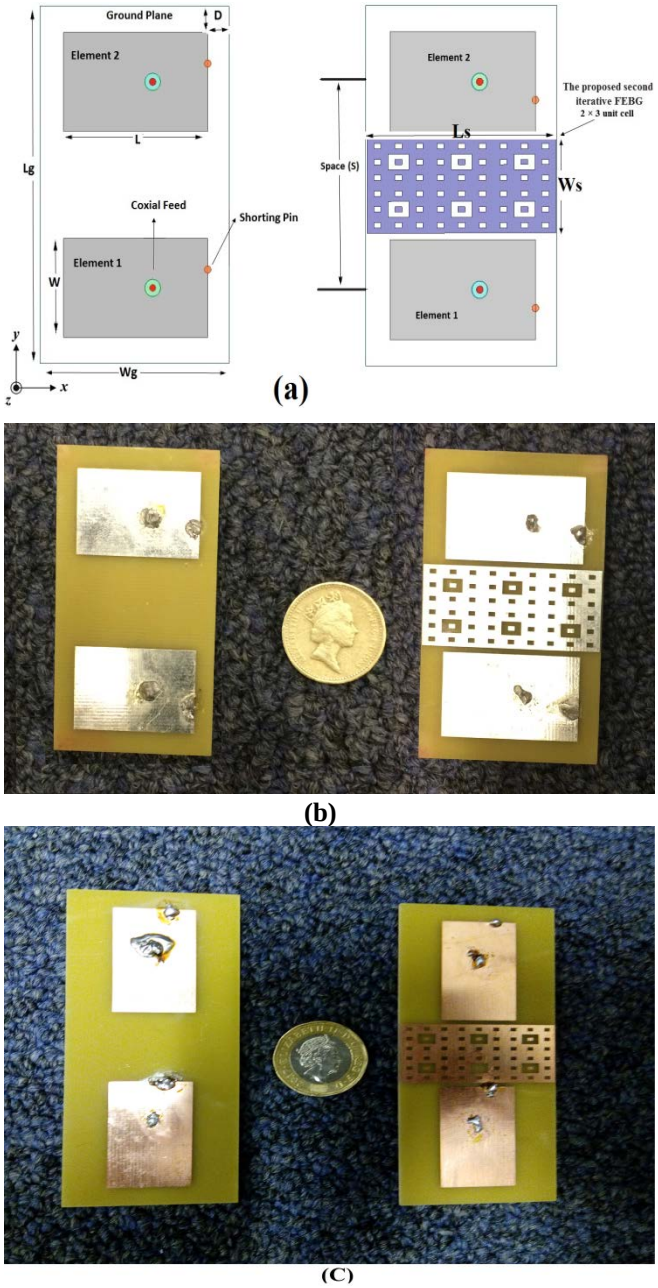

Fig. 3 *configuration of the PIFAs antenna without (left) and with (right) proposed FEBG structure.* ***(a)*** *Schematic antenna layout* ***(b)*** *Prototype of the antenna in H-plane coupling* ***(c)*** *Prototype of the antenna in E-plane coupling.*

The proposed second iterative order FEBG is etched as planar PEC layer between the PIFAs elements and located above the ground plane (as shown in Fig. 3). The basic structure of the second iterative order FEBG etched between dual antenna elements is the same as the fractal geometry illustrated in Fig. 1(*c*). It consists of 2 × 3 periodic unit cells forming a compact lattice (*Ls* × *Ws*). The mutual coupling reduction characteristic of the proposed second iterative order FEBG can be analysed by calculating S_{12} or S_{21} of the antenna array as presented in next section.

3. Performance of the multiple antennae with FEBG structure

3.1. Simulated scattering parameters

The return loss (reflection coefficient) and transmission loss (coupling) for the dual antenna array elements are plotted in Fig. 4(*a*) and Fig. 4(*b*); respectively, in both without and with the proposed second iterative order FEBG structure, the spacing between these antennas is *S* = 40 mm from element centres (corresponding to $0.35\lambda_0$ at 2.65 GHz).

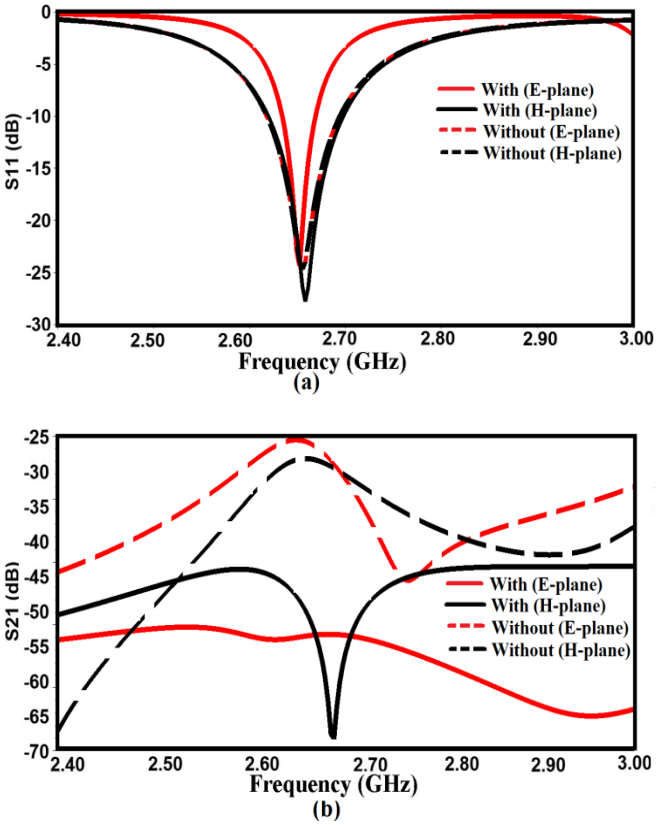

Fig. 4 *the simulated scattering parameters of the antenna without and with second iterative order FEBG structure.* ***(a)*** *Reflection coefficient (S_{11}) and* ***(b)*** *Transmission coefficient (S_{21}).*

Fig. 4(a) illustrates the return loss of adding the second iterative order FEBG between antenna elements. The simulated mutual coupling is significantly reduced as shown in Fig. 4(b), more than 27 dB (*E*-plane) and 40 dB (*H*-plane) coupling reduction have been achieved by inserting second iterative order FEBG structure between the dual antenna elements. All these analyses were conducted with one antenna element transmitting and the other terminated with 50 Ω load.

Analyses were also performed with a lossless substrate with a permittivity of 4.4 to investigate the effects of the lossy substrate. A comparison of the antennas coupling level on lossless and lossy substrates is shown in Fig. 5:-

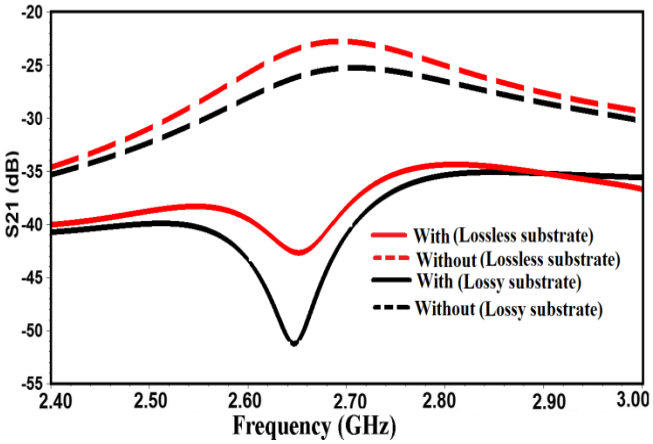

Fig. 5 *coupling level comparison on lossless and lossy substrates.*

Another S_{21} comparison results of the designed zero, first, and second iterative fractal structures (as presented in Fig. 6) shows effect of these structures on the resonant frequency.

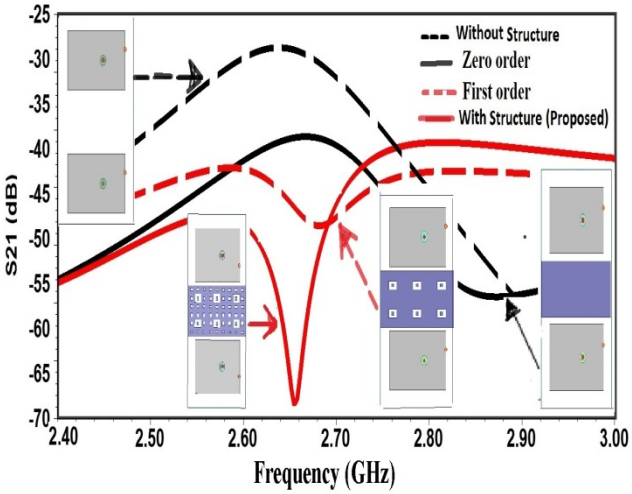

Fig. 6 *S_{21} comparison between different iterative orders FEBG structures (Zero, First and Second).*

Meanwhile, the high-level iterative fractal structure has longer current lines compared with the lower-level iterative fractal structure with the same outline dimension (total size). These results show the significance of using the fractal geometry in a relatively shorter spacing. As the second-order iterative FEBG is inserted (Fig. 6), the electrical length increases, and the stopband frequencies decreases in compared with the zero and first-order iterative FEBG. Although the lower-order fractal EBG is not designed for a working frequency of 2.65 GHz, the first- and second-order iterative fractal structures have explicit bandgap filter components with distinctive characteristics. Therefore, the proposed first and second-order iterative fractal structures can be employed to reduce mutual coupling between the antenna elements. In the present work, the second-order iterative FEBG is taken as an example to illustrate the design procedure of the proposed FEBG for optimum diversity performance.

3.2. Simulated radiation patterns, gain and radiation efficiency

The orientation of the antenna with respect to the coordinate system is shown in Fig. 3. The normalised far-field radiation patterns on *E* and *H* planes are shown in Figs. 7(*a*) and 7(*b*), respectively.
No significant degradation of the radiation patterns is noticed between the designs (with and without the second-order iterative FEBG) of the two orthogonal planes.

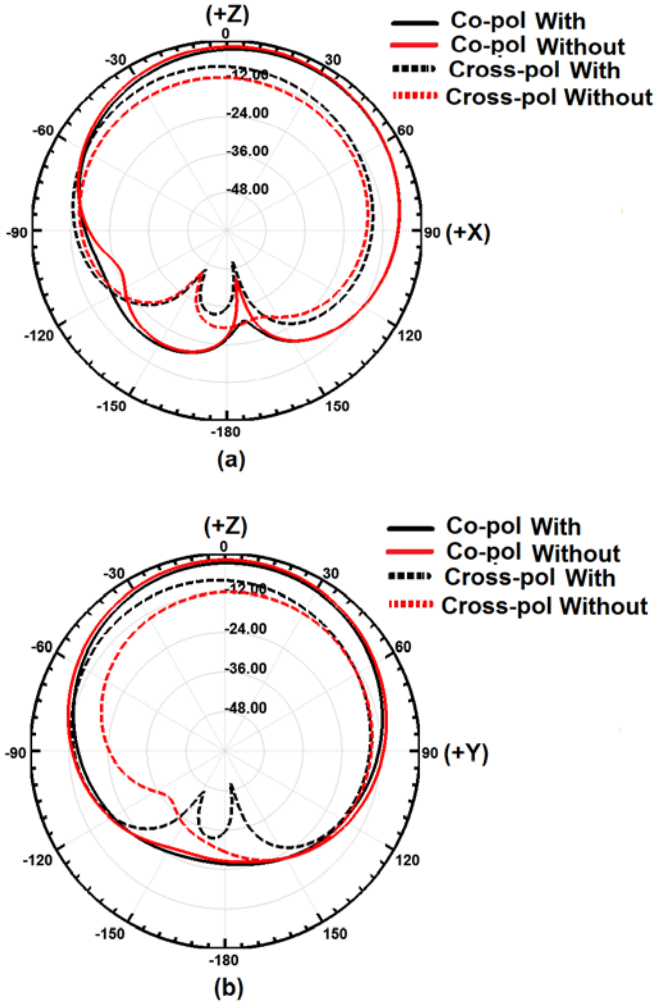

Fig. 7 *the simulated far-field patterns (normalised) with and without second iterative order FEBG at 2.65 GHz.* ***(a)*** *E-plane and* ***(b)*** *H-plane.*

As shown in Fig. 7, the radiation patterns exhibit a good omnidirectional characteristic in the upper semi-plane of E and H planes; thus, the proposed MIMO antenna can transmit and receive signals in a half-sphere perpendicular to the patch. The antenna radiation efficiency is simulated with and without FEBG structure to analyse the effect of the structure on radiation characteristics. Table 2 provides the summarised comparison.

Table 2 Simulated peak gain and radiation efficiency of the proposed antennas

Parameters	Without FEBG	With FEBG
Frequency (GHz)	2.63	2.65
Peak Gain (dB)	1.75	2.57
Radiation Efficiency (%)	64%	68%

Stronger currents on the patches lead to higher energy losses due to lossy substrates. As expected, the inclusion of the FEBG structure has resulted in less mutual coupling and currents on the 2nd antenna. Since the antennas are fabricated on a lossy substrate, the losses induced on the 2nd antenna will be less with low coupling currents leading to higher radiation efficiency with the FEBG structure.

3.3. Diversity performance

The Envelope Correlation Coefficient (ECC) between antenna elements is one of the most important parameters to evaluate diversity performance because it is directly related to the antenna scattering parameters and may significantly degrade MIMO system performance. For dual antenna elements, the envelope correlation coefficient equation using the scattering parameters is given by [11].

$$\rho_{12} = \frac{|S^*_{11}S_{21} - S^*_{12}S_{22}|^2}{(1-|S_{11}|^2-|S_{21}|^2)(1-|S_{22}|^2-|S_{12}|^2)} \qquad (1)$$

In this work, ECC was calculated according to (1) based on assumptions: antenna system is lossless, and the antennas are excited separately, keeping the other antennas matched terminated.

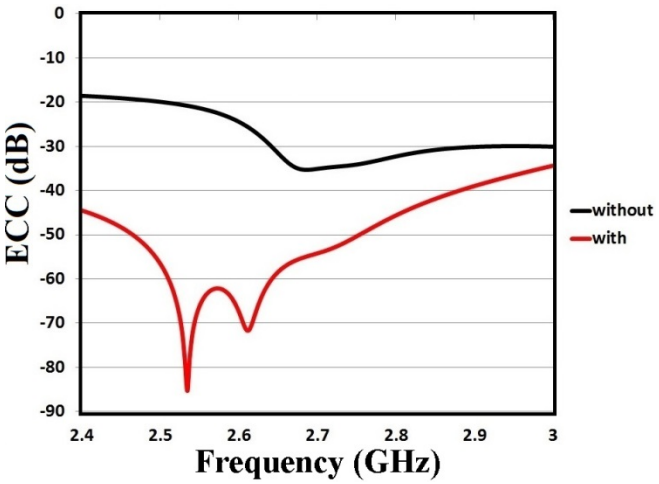

Fig. 8 *Envelope correlation coefficient of MIMO antenna with and without FEBG (H-plane coupling).*

In Fig. 8; the envelope correlation coefficient for the antenna elements with and without the second iterative FEBG is shown against frequency. From the simulated results, the envelope correlation coefficient in the working band of antenna elements with FEBG is -70 dB smaller than that of the antenna elements without FEBG.
This observation indicates better behaviour and diversity performance of MIMO antenna system will be achieved by using the proposed second iterative FEBG.

4. Experimental demonstration

4.1. Measured scattering parameters

The proposed antenna in both scenarios (with and without FEBG structure) was fabricated, tested, measured, and compared with the simulated results for validation.

The return and transmission losses were measured using the Agilent N5230A vector network analyser. Fig. 9(a) shows the measured return loss of the impedance bandwidth (S11 < −10 dB).The proposed antennas resonate at 2.65 GHz with a return loss higher than 10 dB, which corresponds to an impedance bandwidth of 3.16% for both cases.

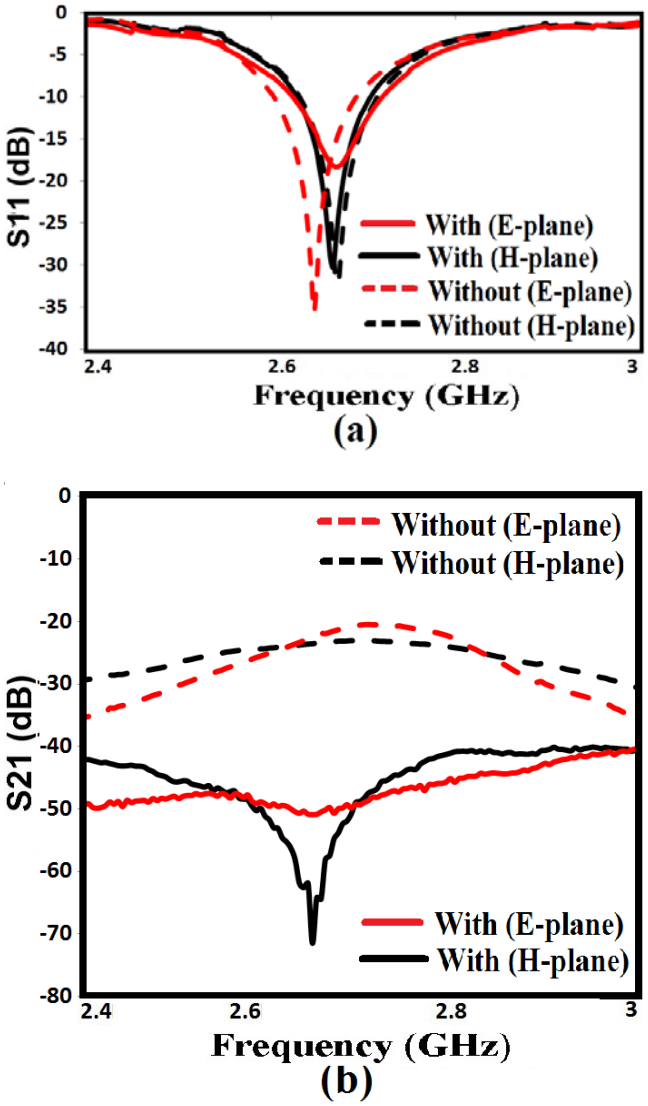

Fig. 9 *Measured scattering parameters of the antenna without and with second iterative order FEBG structure.* ***(a)*** *Reflection coefficient (S_{11}) and* ***(b)*** *Transmission coefficient (S_{21}).*

Figure 9(b) shows the measured mutual coupling between antennas without the FEBG structure which is only -20 dB (*E*-plane) and -25 dB (*H*-plane). After inserting the structure to be significantly reduced to levels: -51 dB (*E*-plane) and -70 dB (*H*-plane). These measured results agree well with the simulated results (as previously shown in Fig. 4). However; a significant agreement exists between the measured and simulated S-parameters results.

A slight difference between these results may be attributed to the common factors, such as inaccuracy in the fabrication process, inappropriate quality of the substrate, and the effect of the SMA connector (solder roughness).

From this experimental verification, it can be concluded that the second iterative order FEBG structure can be utilised to reduce the mutual coupling between antenna array elements.

4.2. Measured and simulated radiation patterns

The measured and simulated far-field radiation patterns are normalised in the two principal planes (*E* and *H*) in both prototypes, without and with the second-order iterative FEBG at a designed frequency of 2.65 GHz, as shown in Figs. 10(*a*-*b*) and 10(*c*-*d*), respectively.

The measured radiation pattern data obtained from the anechoic chamber were relatively few.

Hence, relative radiation patterns were employed for comparison. These values were normalised to the maximum co-pol for comparison with the simulation results.

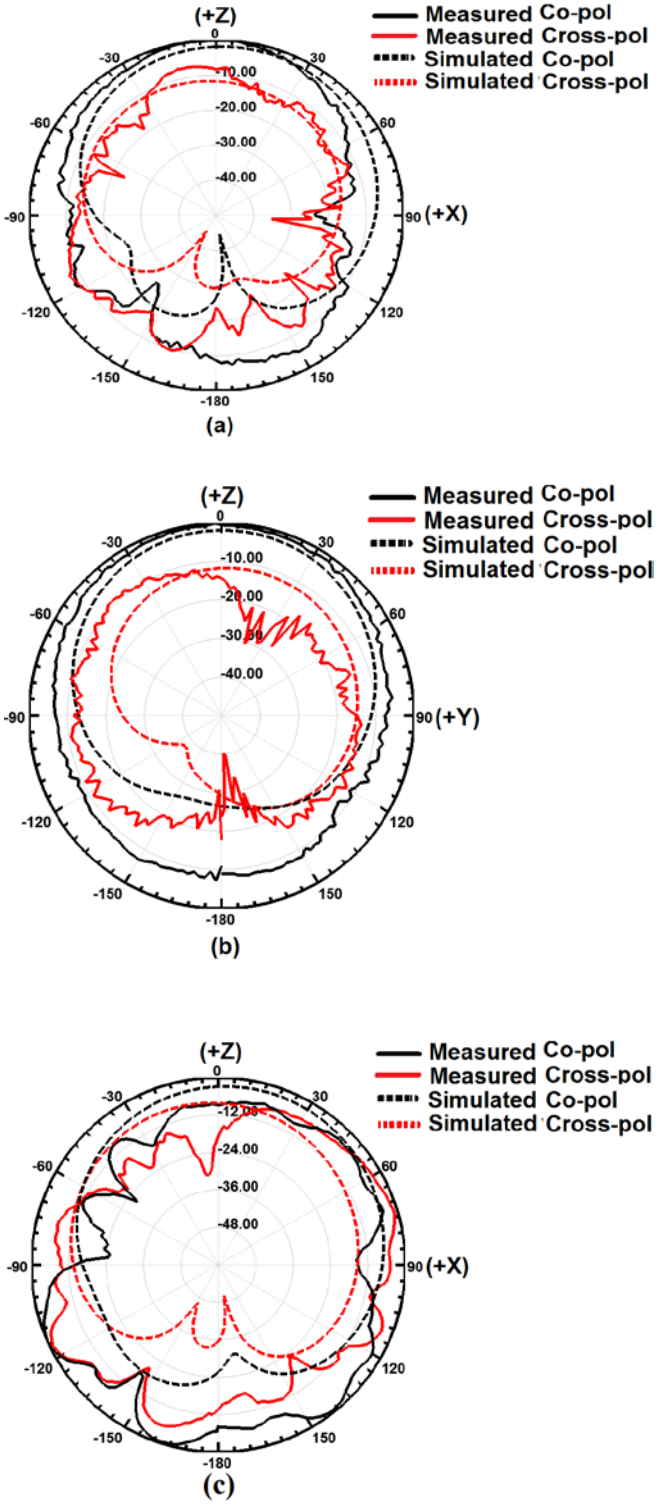

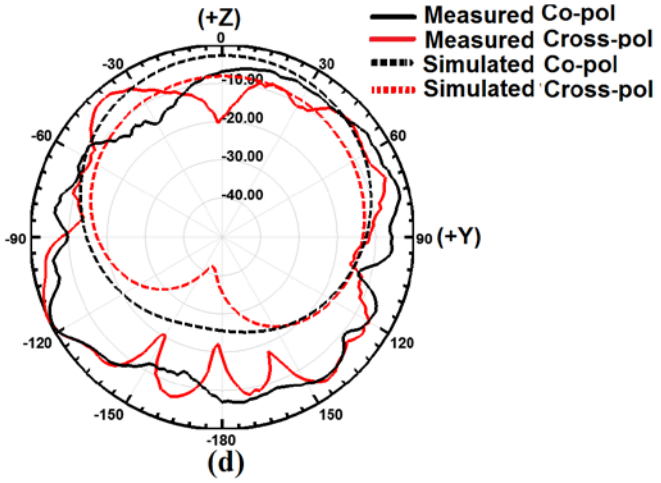

Fig. 10 *Measured versus simulated Co-Pol and X-Pol far-field relative radiation patterns (normalised) at frequency of 2.65 GHz for* ***(a)*** *E-plane (without FEBG),* ***(b)*** *H-plane (without FEBG,* ***(c)*** *E-plane (with FEBG) and* ***(d)*** *H-plane (with FEBG).*

The whole figures of the obtained radiation patterns are acceptable and suitable for modern communication systems. The radiation patterns possess a good omnidirectional characteristic in the upper semi-plane, at the *E* and *H* planes. A large cross-polarisation is observed from the patterns. This characteristic can be an advantage for the wireless communication application in a rich multipath environment. However, probes are used in the present work due to its vertical portion. A large amount of leak and spurious radiation from the probes are produced inside the FR_4 substrate. Therefore, a low XPD level or a high cross-polarisation level is observed. Moreover, discrepancies between the calculated and measured results in the band of interest exist due to the SMA connectors, cable losses, and inaccurate implementation. In addition; an imperfect placement/connection of shorting pins or via during the fabrication and measurements process must have contributed towards the discrepancies between measured and simulated patterns. The ground surface waves can produce more spurious radiations or couple some energy at imperfectly placed shorting pins, feed connections for PIFA probes or any other discontinuities, which in turn will lead to some distortions in the main patterns or unwanted loss of power. Authors believe that this is one of the reasons that had been lead to this discrepancy, especially in the measured results. Finally; during the measurements, one of the input ports was excited, and the other was terminated with a load of 50 Ω.

5. Comparison of FEBG structure with other approaches and previous work

It is instructive to compare the proposed FEBG structure with other methods used to reduce the mutual coupling. To reduce the mutual coupling between antenna elements, besides FEBG, different approaches such as removal of the both substrate and common ground have also been reported [35]. Fig. 11 plots the coupled antenna structures to be compared:

a) Normal antennas (reference).
b) Substrate between antennas removed.
c) The ground between antennas removed,
d) FEBG structure between antennas.

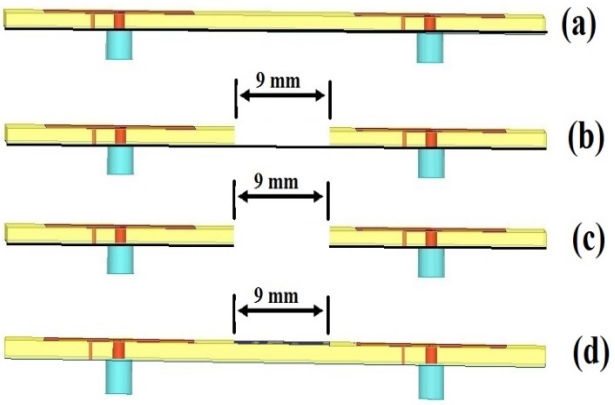

Fig. 11 *Other techniques to reduce the mutual coupling between PIFAs (Side view):* ***(a)*** *Normal antennas,* ***(b)*** *Substrate between antennas removed,* ***(c)*** *The ground between antennas removed, and* ***(d)*** *FEBG structure in between.*

All physical parameters such as antenna size, substrate properties, and antenna distance in all the structures were kept identical to the second iterative order FEBG case.

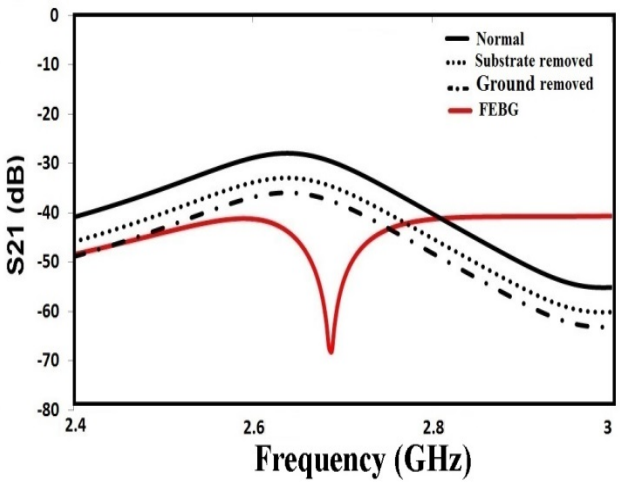

Fig. 12 *Mutual coupling comparison of the four different techniques. PIFA antennas resonate at 2.65 GHz.*

A 9 mm substrate width was removed between the antennas (as illustrated in Fig. 11(b)); this width is chosen to be the same as the total width of rows of the FEBG patches. When the ground was removed between the antennas, the separation between adjacent patch antennas was also selected to be 9 mm (as illustrated in Fig. 11(c)). Figure 12 displays the mutual coupling reduction results of four different approaches.

The conventional antennas show the highest coupling. The substrate and ground removal cases have some effects on the mutual coupling reducing. A 5 dB coupling reduction is noticed for the former case, and an 8 dB reduction is observed for the latter case. The highest mutual coupling

reduction is seen with the second iterative order FEBG case compared to other approaches (as presented in Fig. 12).

This comparison demonstrates the unique capability of the FEBG structure to reduce the mutual coupling.
Moreover, as mentioned before, some other published works have employed different methods such as EBG and DGS structures, slotted and slits ground plane, resonators and neutralisation technique to reduce the mutual coupling between antenna elements. A summarized comparison is provided in Table 3 of the manuscript.

Table 3 Performance comparison of different planar multiple antennas

Ref	BW (GHz)	S_{21} With case (dB)		S_{21} Without case (dB)		Space (λ_0)	Volume (mm^3)	Isolation technique	Geometric complexity
		E	H	E	H				
[4]	1.92-2.18	-27	NA	-10	NA	0.13	100×40×5	Neutralisa-tion line	Complex
[13]	2.5-2.58	-29	-32	-20	-18	0.50	100×40×3	Dual Layer EBG	Complex
[15]	1.85-2.15	-27	NA	-9.4	NA	0.50	100×40×2	Slits on ground	Medium
[17]	2.42-2.59	-28	NA	-10	NA	0.17	100×40×5	Parasitic ground	Medium
[19]	2.55-2.75	-32	-40	-22	-24	0.40	75×65×5	Walls in between	Medium
[20]	2.40-2.65	-16	-20	-8	-9.5	0.42	105×55×5.7	Good separation	Simple
[23]	2.32-2.68	-38	NA	-18	NA	0.15	100×40× 5	Slot in between	Complex
[30]	2.38-2.47	-22	NA	-13	NA	0.12	100×50×6.5	Planner EBG	Complex
This work	2.64-2.68	-52	-67	-25	-27	0.35	68×40×1.6	Compact FEBG	Simple

6. Conclusion

A novel planar fractal-based EBG structure has been proposed in this paper for mutual coupling reduction between dual microstrip antennas (PIFAs) elements for MIMO applications (working at LTE radio frequency of 2.65 GHz).Second iterative order FEBG with bandgap filter characteristic was employed to reduce mutual coupling between dual PIFAs elements due to its capability of suppressing surface waves propagation in a given frequency range. All the simulations were carried out using Ansoft HFSS ver 17.0 (High-Frequency Simulator Structure).
The designed antenna was fabricated and measured to verify the simulated results. The measured and simulated results of the scattering parameters and far-field radiation patterns showed excellent agreement. A high coupling reduction of more than 27 dB (*E*-plane) and 40 dB (*H*-plane) has been achieved between the dual antennas for an antenna spacing less than $0.35\lambda_0$ without much degradation of the radiation characteristics. Meanwhile, the diversity performance of the proposed antenna system can be improved due to the reduction of Envelope Correlation Coefficient (ECC) resulted from the suppression of the mutual coupling.
Therefore; the proposed antenna with fractal-based EBG structure (FEBG) is shown to be useful for low-frequency narrow-band MIMO/diversity applications.

7. References

[1] C. A. Balanis, Antenna Theory: Analysis and Design, 3rd Edition. Hoboken, NJ: John Wiley & Sons, Inc., 2005.

[2] S. D. Assimonis, T. V. Yioultsis, and C. S. Antonopoulos, "Design and Optimization of Uniplanar EBG Structures for Low Profile Antenna Applications and Mutual Coupling Reduction," IEEE Transactions on Antennas and Propagation, vol. 60, no. 10, pp. 4944–4949, 2012.

[3] L. Yang, T. Li, and S. Yan, "Highly Compact MIMO Antenna System for LTE/ISM Applications," International Journal of Antennas and Propagation, vol. 2015, pp. 1–10, 2015.

[4] A. Diallo, C. Luxey, P. L. Thuc, R. Staraj, and G. Kossiavas, "Study and Reduction of the Mutual Coupling Between Two Mobile Phone PIFAs Operating in the DCS1800 and UMTS Bands," IEEE Trans. Antennas Propagat. IEEE Transactions on Antennas and Propagation, vol. 54, no. 11, pp. 3063–3074, 2006.

[5] F. Yang and Y. Rahmat-Samii, "Microstrip antennas integrated with electromagnetic band-gap (EBG) structures: A low mutual coupling design for array applications," IEEE Transactions on Antennas and Propagation, vol. 51, no. 10, pp. 2936–2946, 2003.

[6] Y. Su, L. Xing, Z. Z. Cheng, J. Ding, and C. J. Guo, "Mutual coupling reduction in microstrip antennas by using dual layer uniplanar compact EBG (UC-EBG) structure," 2010 International Conference on Microwave and Millimeter Wave Technology, 2010.

[7] B.-Q. Lin, Q.-R. Zheng, and N.-C. Yuan, "A novel planar PBG structure for size reduction," IEEE Microwave and Wireless Components Letters, vol. 16, no. 5, pp. 269–271, 2006.

[8] K. Wei, J.-Y. Li, L. Wang, Z.-J. Xing, and R. Xu, "Mutual Coupling Reduction by Novel Fractal Defected Ground Structure Bandgap Filter," IEEE Transactions on Antennas and Propagation, vol. 64, no. 10, pp. 4328–4335, 2016.

[9] Y. Hajilou, H. R. Hassani, and B. Rahmati, "Mutual coupling reduction between microstrip patch antennas," 2012 6th European Conference on Antennas and Propagation (EUCAP), 2012.

[10] M. K. Meshram, R. K. Animeh, A. T. Pimpale, and N. K. Nikolova, "A Novel Quad-Band Diversity Antenna for LTE and Wi-Fi Applications With High Isolation," IEEE Trans. Antennas Propagat. IEEE Transactions on Antennas and Propagation, vol. 60, no. 9, pp. 4360–4371, 2012.

[11] J. Byun, J.-H. Jo, and B. Lee, “Compact dual-band diversity antenna for mobile handset applications,”Microwave and Optical Technology Letters, vol. 50, no. 10, pp. 2600–2604, 2008.

[12] A. Chebihi, C. Luxey, A. Diallo, P. L. Thuc, and R. Staraj, “A Novel Isolation Technique for Closely Spaced PIFAs for UMTS Mobile Phones,” IEEE Antennas and Wireless Propagation Letters, vol. 7, pp. 665–668, 2008.

[13] S. Ghosh, T.-N. Tran, and T. Le-Ngoc, “Dual-Layer EBG-Based Miniaturized Multi-Element Antenna for MIMO Systems,” IEEE Trans. Antennas Propagat. IEEE Transactions on Antennas and Propagation, vol. 62, no. 8, pp. 3985–3997, 2014.

[14] C.-Y. Chiu, C.-H. Cheng, R. D. Murch, and C. R. Rowell, “Reduction of Mutual Coupling Between Closely-Packed Antenna Elements,” IEEE Transactions on Antennas and Propagation, vol. 55, no. 6, pp. 1732–1738, 2007.

[15] A. P. Feresidis and Q. Li, "Miniaturised slits for decoupling PIFA array elements on handheld devices," Electron. Lett., vol. 48, pp. 310-312, 2012

[16] T. Fukusako and Y. Harada, “A Comprehensive Study On Decoupling Between Inverted-F Antennas Using Slitted Ground Plane,” Progress In Electromagnetics Research C, vol. 37, pp. 199–209, 2013.

[17] Y. Gao, X. Chen, Z. Ying, and C. Parini, “Design and Performance Investigation of a Dual-Element PIFA Array at 2.5 GHz for MIMO Terminal,” IEEE Trans. Antennas Propagat. IEEE Transactions on Antennas and Propagation, vol. 55, no. 12, pp. 3433–3441, 2007.

[18] S. Zhang, B. K. Lau, Y. Tan, Z. Ying, and S. He, “Mutual Coupling Reduction of Two PIFAs With a T-Shape Slot Impedance Transformer for MIMO Mobile Terminals,”IEEE Trans. Antennas Propagat. IEEE Transactions on Antennas and Propagation, vol. 60, no. 3, pp. 1521–1531, 2012.

[19] J.-Y. Pang, S.-Q. Xiao, Z.-F. Ding, and B.-Z. Wang, “Two-Element PIFA Antenna System With Inherent Performance of Low Mutual Coupling,” Antennas Wirel. Propag. Lett. IEEE Antennas and Wireless Propagation Letters, vol. 8, pp. 1223–1226, 2009.

[20] S. Ghosh, T.-N. Tran, and T. Le-Ngoc, “Miniaturized Four-Element Diversity PIFA,”Antennas Wirel. Propag. Lett. IEEE Antennas and Wireless Propagation Letters, vol. 12, pp. 396–400, 2013.

[21] S. A. Ja'afreh, Y. Huang, and L. Xing, “Low profile and wideband planar inverted-F antenna with polarisation and pattern diversities,” IET Microwaves, Antennas & Propagation, vol. 10, no. 2, pp. 152–161, 2016.

[22] N. H. Noordin, Y. C. Wong, A. T. Erdogan, B. Flynn, and T. Arslan, “Meandered inverted-F antenna for MIMO mobile devices,” 2012 Loughborough Antennas & Propagation Conference (LAPC), 2012.

[23] S. Zhang, S. N. Khan and S. He, "Reducing mutual coupling for an extremely closely-packed tunable dual-element PIFA array through a resonant slot antenna formed in-between," IEEE Transactions on Antennas and Propagation, vol. 58, pp. 2771-2776, 2010.

[24] Ó. Quevedo-Teruel, L. Inclan-Sanchez and E. Rajo-Iglesias, "Soft Surfaces for Reducing Mutual Coupling Between Loaded PIFA Antennas," in IEEE Antennas and Wireless Propagation Letters, vol. 9, no. , pp. 91-94, 2010.

[25] Y. Wang, J. Huang, and Z. Feng, “A novel fractal multi-band ebg structure and its application in multi-antennas,” 2007 IEEE Antennas and Propagation International Symposium, 2007.

[26] H. Farahani, M. Veysi, M. Kamyab, and A. Tadjalli, “Mutual Coupling Reduction in Patch Antenna Arrays Using a UC-EBG Superstrate,” IEEE Antennas and Wireless Propagation Letters, vol. 9, pp. 57–59, 2010.

[27] J. D. D. Ruiz, F. L. Martinez, and J. Hinojosa, “Novel Compact Wide-Band EBG Structure Based on Tapered 1-D Koch Fractal Patterns,” IEEE Antennas and Wireless Propagation Letters, vol. 10, pp. 1104–1107, 2011.

[28] Wang, Haiming, et al. "A high isolation MIMO antenna used a fractal EBG structure." Antennas & Propagation (ISAP), 2013 Proceedings of the International Symposium on. Vol. 1. IEEE, 2013.

[29] J. Guterman, A. Moreira, and C. Peixeiro, “Two-element multi-band fractal PIFA for MIMO applications in small size terminals,” IEEE Antennas and Propagation Society Symposium, 2004., 2004.

[30] Z. Z. Abidin, R. A. Abd-Al Hameed, N. J. Mcewan, and M. B. Child, “Analysis of the effect of EBG on the mutual coupling for a two-PIFA assembly,” 2010 Loughborough Antennas & Propagation Conference, 2010.

[31] D. Sievenpiper, L. Zhang, R. Broas, N. Alexopolous, and E. Yablonovitch, “High-impedance electromagnetic surfaces with a forbidden frequency band,” IEEE Transactions on Microwave Theory and Techniques IEEE Trans. Microwave Theory Techn., vol. 47, no. 11, pp. 2059–2074, 1999.

[32] P. Kovacs, T. Urbanec "Electromagnetic Bandgap Structures: Practical Tips and Advice for Antenna Engineers," Radioengineering, Vol. 21, No.I, pp. 414-421, Apr 2012.

[33] A. H. Radhi, N. A. Aziz, R. Nilavalan, and H. S. Al-Raweshidy, “Mutual coupling reduction between two PIFA using uni-planar fractal based EBG for MIMO application,” 2016 Loughborough Antennas & Propagation Conference (LAPC), 2016.

[34] F. Yang and Y. Rahmat-Samii, “Electromagnetic Band Gap Structures in Antenna Engineering,” 2008.

[35] M. Salehi and A. Tavakoli, “A novel low mutual coupling microstrip antenna array design using defected ground structure,” AEU-International Journal of Electronics and Communications, vol. 60, no. 10, pp. 718–723, 2006.